Linear and Nonlinear Optical Characterization of Dye–Polymer Composite Films Based on Methylcellulose Incorporated with Varying Content of Methylene Blue

Omed Gh. Abdullah[1] · Dler M. Salh[2] · Azhin H. Mohamad[3] · Gelas M. Jamal[1] · Hawzhin T. Ahmed[4] · Bakhan S. Mustafa[5] · Mahdi H. Suhail[6]

Abstract

Compositional dependence of the linear and nonlinear optical characteristics of dye–polymer composite (DPC) films based on methylcellulose-methylene blue (MC-MB) were studied. The absorbance spectra were used to estimate absorption edge, optical density, skin depth, optical band gap energy, and Urbach's parameters for all DPC films. The direct allowed optical band gap energy decreased from 6.29 eV for pure MC to 5.95 eV when doped with 2.5 wt.% of MB. The dispersion of the refractive index is discussed in terms of both the single-oscillator Wemple–DiDomenico and single Sellmeier oscillator models. The nonlinear optical characteristics such as the third-order nonlinear optical susceptibility and nonlinear refractive index were calculated using the dispersive oscillator parameters obtained from the single-oscillator model. The observed improvements in the linear and nonlinear optical characteristics of MC upon incorporating MB make the present DPC a potential candidate for multifunctional applications like optoelectronic and photonic devices.

Keywords Absorption edge · optical bandgap energy · methylene blue · nonlinear optic

Introduction

Nowadays, polymer composite materials have received the prestigious attraction of many researchers and practitioners owing to their unique and interesting properties as well as due to their potential applications in modern technology and industry, where they can be used in numerous electronics, optics, and optoelectronic devices operating in the ultraviolet, visible, and near-infrared ranges.[1–4] It is being reported that the optical bandgap of the polymer matrix can be tuned upon the addition of a small amount of suitable additive, so the polymer composites are more appropriate for various optoelectronic devices covering wide ranges of electromagnetic radiation.[5] The optical and electrical properties of different polymer composite films have been extensively studied because they can be controlled in sample preparation to meet the specific requirements of different applications, with desirable properties which are not present in the parent materials.[6,7]

Dyes are unsaturated organic compounds with a complex aromatic molecular structure that emit bright colors.[6] The aromatic molecular structures of dyes make the host polymer of the dye-polymer composite (DPC) more stable. Organic dyes have a wide spectral range in the visible region, allowing concentration and hence absorption to be easily controlled, making DPC suitable in a variety of applications in the field of sensors and information displays due to the largest variations in the optoelectronic properties of the dyes.[8] The most common host materials

✉ Omed Gh. Abdullah
omed.abdullah@univsul.edu.iq

1   Advanced Materials Research Laboratory, Department of Physics, College of Science, University of Sulaimani, Sulaymaniyah, Kurdistan Region 46001, Iraq

2   Department of Chemistry, College of Science, University of Sulaimani, Sulaymaniyah, Kurdistan Region 46001, Iraq

3   Department of Physics, College of Education, University of Sulaimani, Sulaymaniyah, Kurdistan Region 46001, Iraq

4   Department of General Science, College of Education and Language, Charmo University, Chamchamal, Sulaimani, Kurdistan Region 46023, Iraq

5   Department of Physics, College of Science, University of Halabja, Halabja, Kurdistan Region 46006, Iraq

6   Department of Physics, College of Science, University of Baghdad, Baghdad 10001, Iraq

utilized to make DPC were polymethyl methacrylate (PMMA) and polyvinyl alcohol (PVA).[9]

Ghoshal et al.[10] used methylene blue (MB) dye to modify the properties of PVA and found that the addition of MB reduced the crystallinity of the PVA host. The optical properties of the system were improved, and the bandgap was reduced as a result of the interaction between the PVA and the dye molecule.

Methylcellulose (MC) is water-soluble, derived from long-chain cellulose, with excellent film-forming characteristics. Due to several advantages, such as biocompatibility, biodegradability, abundance in nature, very low cost, water-solubility, nontoxic nature, and dopant-dependent properties, MC has a wide range of applications depending on its degree of substitution.[11–13] On the other hand, MB is a cationic thiazine dye having a heterocyclic aromatic chemical compound with the molecular formula $C_{16}H_{18}N_3SCl$. In addition, MB dye has several advantages: it is low-cost, water-soluble, and does not precipitate.[14]

In the present work, the effect of photosensitizer MB dye concentration on the optical parameters of MC matrix was investigated, including some topics and issues that have not been exposed to study in the previous literature, such as optical density, skin depth, Urbach's parameters, and the dispersion parameters as a function of MB content.

Experimental Details

Dye polymer composite films have been prepared by the conventional solution casting-evaporation technique. MC ($C_{29}H_{54}O_{16}$) and MB ($C_{16}H_{18}ClN_3S$) were used to synthesize the DPC films with varying MB compositions from 0.5 wt.% to 2.5 wt.%. Different compositions of DPCs were prepared by dissolving 6 g of MC in 240 ml double-distilled water at room temperature using a magnetic stirrer. MB in appropriate weight percentages was added to pure MC solution with continuous stirring. The homogeneous solutions of DPCs were cast into clean Petri plates and allowed to solidify by slow evaporation of the solvent to form films. The prepared DPC films were placed in the desiccators for further drying prior characterizations. To achieve uniform films, the same conditions were applied to all samples during preparation. The prepared samples had film thicknesses ranging from 29 μm to 33 μm. It is worthy to mention that, the colors of these DPC films have changed from white to light blue solution and finally they became dark blue at the highest MB content.

A PerkinElmer Lambda 25 double-beam UV-visible spectrophotometer was used. The spectrum measurements were recorded in the absorbance mode in the spectral wavelength range of 190–1100 nm.

Results and Discussion

Optical Absorption Coefficient

The optical behaviors of certain polymeric materials depend on parameters such as the preparation conditions, surface morphology, dopant materials, and their concentration.[15] The study of the absorption coefficient spectra of any polymer composite materials gives decent information about the electronic states of the system. Based on the optical absorption response, DPCs have several applications like solar cells, sensors, photoelectrochemistry, optoelectronics, and display devices.[16] Therefore, the optical absorbance (A) and the optical absorption coefficient (α) spectra for all prepared DPCs have been studied here. The α with the function of λ was determined from the measured A spectra using the formula ($\alpha(\lambda) = 2.303A(\lambda)/t$),[17] where t is the film thickness.

The typical absorbance spectrum of pure photosensitizer MB is shown in Fig. 1. The inset describes the structure of MB. The UV–visible spectra of aqueous MB displays five maximal absorption peaks at 247, 292, 334, 613, and 664 nm, which is in accordance with that reported previously.[18–20] The two major absorbance peaks at 292 and 664 nm are due to the benzene ring and heteropolyaromatic linkage. In addition, the double-peak feature at 613 nm and 664 nm corresponds to the dimeric and monomeric form of MB, respectively, and the characteristic band of MB at 292 nm corresponds to $\pi \rightarrow \pi^*$ transitions.[19]

The dependence of $\alpha(\lambda)$ of MC-MB DPC films on the incident wavelength for different MB content is depicted in Fig. 2. The analysis of the figure shows that the value of $\alpha(\lambda)$ increases gradually with the increase in MB in the system in the certain wavelength range 190–692 nm; beyond this wavelength, i.e. in the near-infrared region, $\alpha(\lambda)$ becomes invariant. This is due to the absorbing nature of the MB. Since MC is a colorless polymer, it does not have any absorption of visible light in the 300–700 nm region.[21]
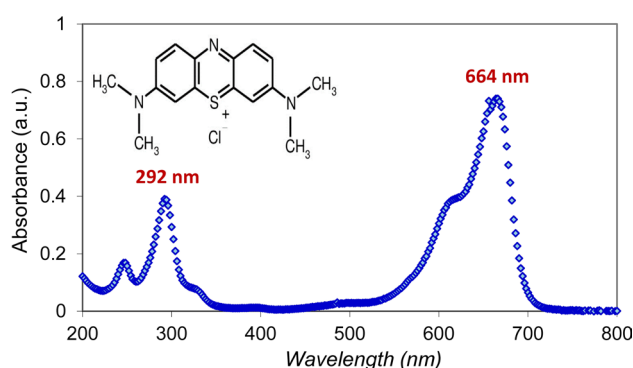

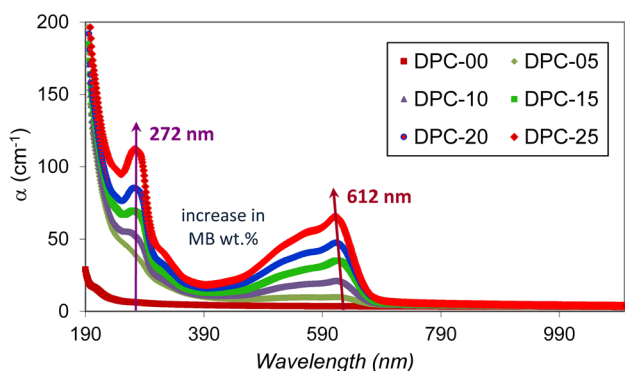**Fig. 1.** The optical absorbance spectra for pure photosensitizer methylene blue (MB).

Fig. 2. The variation of the optical absorption coefficient of MC-MB DPC films with the incident wavelength.

Fig. 3. The variation of the optical density (D_{opt}) with the incident photon energy for MC-MB DPC films.

The UV–vis spectra of the MC-MB DPC films exhibit two maximum peaks at 272 nm and 612 nm which are respectively 20 nm and 52 nm blue-shifted as compared to the absorption peaks of aqueous MB (at 292 nm and 664 nm). This shift in the absorption bands and band edges due to an increase in MB could be ascribed to the formation of intermolecular hydrogen bonding of the MB with the OH groups of the MC matrix.[22] According to Gao et al.,[23] phenothiazine dyes like MB suffer from a blue-shift absorption band as a result of H-aggregate formation through π–π stacking of the molecules.

The onset of the absorption edge has been determined for each sample and it was observed that all values are located in the IR region. It was observed that the onset of the absorption edge was shifted towards longer wavelengths as the MB content was increased from $\lambda = 200$ nm (6.2 eV) for pure MC to $\lambda = 217$ nm (5.7 eV) for DPC loaded 2.5 wt.% MB. This shift is to be expected, as it shows a decrease in the optical band gap energy as the MB concentration in the system increases. These findings are consistent with previous studies on a variety of polymer composites.[24]

On the other hand, the optical density (D_{opt}) of the present MC-MB DPC films was calculated by multiplying the absorption coefficient with file thickness ($D_{opt} = \alpha d$).[25] Figure 3 depicts the variation of the D_{opt} with the incident photon energy ($h\nu$). Because all samples have nearly identical thicknesses, the variation of the D_{opt} is analogous to the behavior of the absorption coefficient.

The Skin Depth of DPC Films

The absorption of the electromagnetic spectrum with film texture is dependent on many important parameters, including the material type, thickness, skin thickness, optical conductivity, and dopant types and their ratios.[25,26] Due to a variety of factors, such as film density, refractive index, microstructure, and surface morphology, the photon current
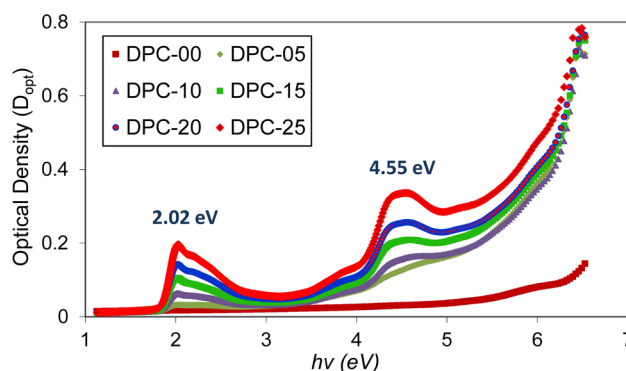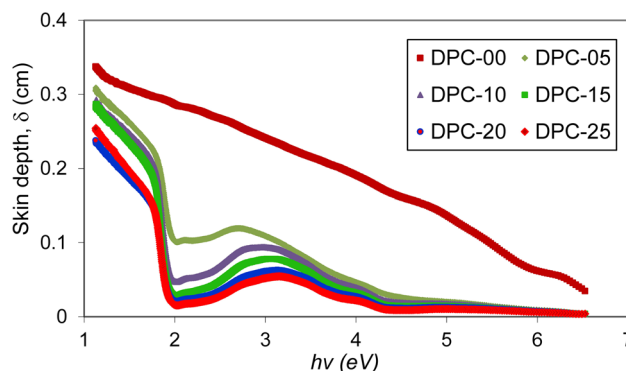

Fig. 4. The variation of the skin depth of pure MC and MC-MB DPC films as a function of the incident photon energy.

density decreases exponentially from the surface to the midway of the films. The thickness at which photon current density decreases by 1/e of the value at the surface is called skin depth or penetration depth (δ). The value of δ also depends on the frequency of incident photons and optical band gap of the film. The δ is related to the α by ($\delta = 1/\alpha$).

The DPC films have a lower skin depth because of their higher optical absorption coefficient in comparison with pure MC, as depicted in Fig. 4, which shows the dependence of δ on the incident photon energy ($h\nu$). Furthermore, the skin depth was found to decrease as the MB content increased. Increasing the concentration of MB causes the DPC films to become darker, resulting in a decrease in the value of transparency for the films, thereby causing the reduction in the skin depth.

Optical Energy Gap

In the high absorption region of semiconductors and amorphous materials, the relation between the absorption coefficient (α) and the incident photon energy ($h\nu$) can be described by using Tauc's relation:[27]

$$\alpha = \frac{\alpha_{\mathrm{o}}\left(hv - E_{\mathrm{g}}\right)^{\gamma}}{hv} \tag{1}$$

where α_{o} is the energy-independent constant, also known as the band tailing parameter, and E_{g} is the optical energy gap located between the localized states near the mobility edges according to Mott and Davis' density of states model.[28] The constant γ in Eq. 1 is the power factor of the transition mode. It depends on the nature of the composition, whether it is crystalline or amorphous, as well as the photon transition. The values of γ are 1/2, 2, 3/2, and 3, for direct allowed, indirect allowed, direct forbidden, and indirect forbidden transitions, respectively.[21]

After plotting $(\alpha hv)^{1/\gamma}$ versus hv for all power probabilities of γ for the present DPC films, it was found that the most suitable and adequate plot is that when $\gamma = 1/2$, as shown in Fig. 5. Therefore, and according to Tauc's equation, the direct allowed optical energy gap (E_{dg}) value of the investigated films was estimated by extending the straight line to intercept the hv-axis.

It was observed that, the E_{dg} decreased with increasing MB content in DPC films from 6.29 eV for pure MC to 5.95 eV when doped with 2.5 wt.% of MB. This can be attributed to the formation of new localized electron states at the defect site within the bandgap as a result of MB loading into the MC matrix. This result was confirmed by an investigation of the band tail width using the empirical Urbach equation in the next section. It is worthy to mention that the polymer composite with fine variation/tunable bandgap properties has many potential applications in photovoltaic and optoelectronic devices.[29]

Absorption Band Tail (Urbach Energy)

The optical absorption spectra of amorphous materials have a significant role because they provide basic information about the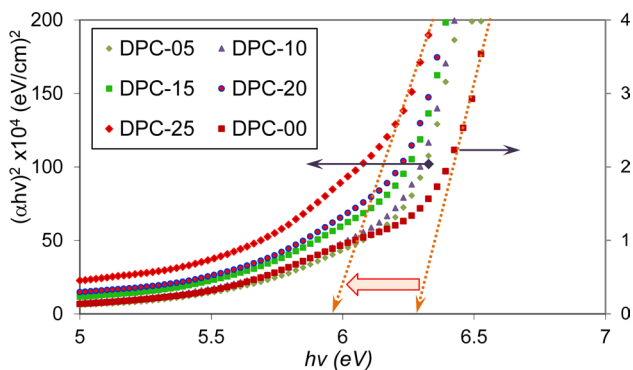ir structure and optical bandgap. In general, the UV-Vis absorption spectra of semiconductors and amorphous materials can be divided into three distinguished regions: (1) weak absorption, which is caused by defects and impurities, (2) absorption edge, which is caused by the disorder and structural perturbation, and (3) strong absorption that defines the optical band gap energy.[30]

Along the absorption coefficient curve and near the absorption edge, there is an exponential part called the Urbach tail. This exponential tail appears in disordered and amorphous materials because these materials have localized states that extend within the normal bandgap. In this range, the absorption coefficient (α) versus photon energy (hv) follows the Urbach empirical rule given by the following equation:[31]

$$\alpha = \alpha_{\mathrm{o}} \exp\left(\frac{hv}{E_{\mathrm{U}}}\right) \tag{2}$$

where α_{o} is a constant and E_{U} represents the energy of the band tail width or Urbach energy, which identifies the localized states associated with disordered that are weakly temperature-dependent.

A straight line equation can be obtained by taking the natural logarithm of Eq. 2, expressed as follows:

$$\ln \alpha = \ln \alpha_{\mathrm{o}} + \frac{hv}{E_{\mathrm{U}}} \tag{3}$$

The value of E_{U} can be obtained from the slope of the straight line of the Urbach plot ($\ln \alpha$ versus hv) for all prepared samples as shown in Fig. 6. The best straight line fitting results confirm that the present DPC films obey the Urbach empirical rule due to the amorphous nature of the system. A slope of the Urbach graph is equal to $1/E_{\mathrm{U}}$ and the intercept on the y-axis is equal to $\ln\left(\alpha_{\mathrm{o}}\right)$. The observed increase in Urbach energy of the present DPC films from 1.03 eV for pure MC to 1.10 eV, 1.18 eV, 1.27 eV, 1.30 eV, and 1.37 eV as the MB content increases respectively to 0.5 wt.%, 1.0 wt.%, 1.5 wt.%, 2.0 wt.%, and 2.5 wt.%, suggested
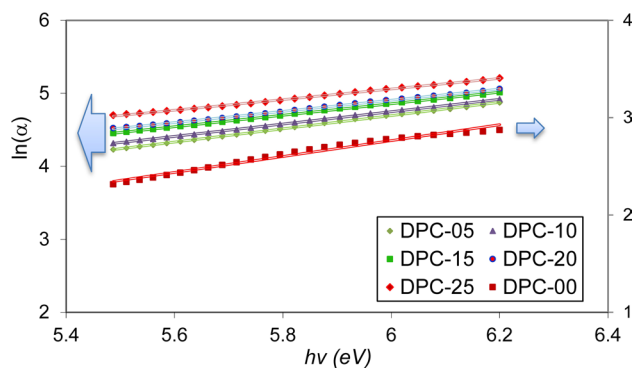

Fig. 5. Dependence of $(\alpha hv)^2$ of MC-MB DPC films upon the incident photon energy .(hv)

Fig. 6. The dependence of $\ln(\alpha)$ for the MC-MB DPC films upon the photon energy (hv), to calculate the Urbach energy.
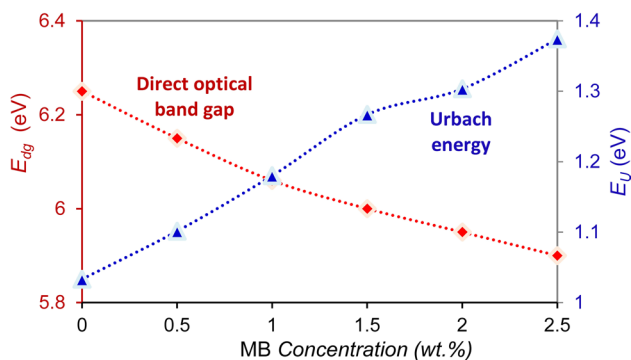
Fig. 7. Dependence of the direct optical energy gap, and the Urbach energy upon the MB concentration in DPC films.
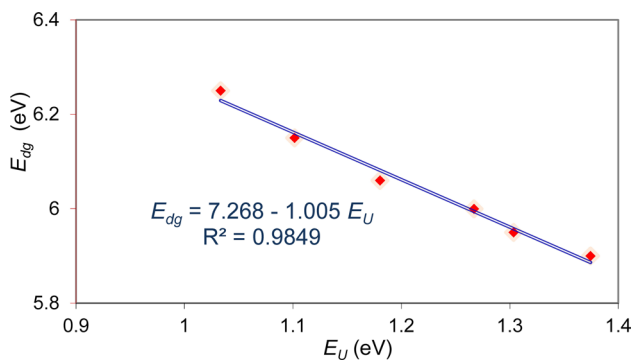

Fig. 8 The relation between direct bandgap energy (E_{dg}) and the width of the Urbach tail (E_U) of MC-MB DPC films.

the creation of new localized states and traps in the bandgap of MC, leading to the observed reduction in E_{dg}. Similar behavior has been reported for different polymer composites with low crystalline phases.[17,29,32–34]

Figure 7 illustrates the dependence of the E_{dg} and E_U on the MB content in the present DPC films. It can be seen that as the MB content in the MC matrix increased, the value of the E_U increased, which is opposite to the behavior of the E_{dg} as seen in Fig. 7. The increase in E_U in response to an increase in MB concentration confirms the increase of the amorphous state in the matrix and the formation of defects in the band structure. Hence, the optical band gap decreases as well.[35]

From Fig. 7, it can be observed that the interrelation between E_{dg} and E_U can be fit to a linear relationship. The empirical equation arising from this linear fitting is: $E_{dg} = 7.268 - 1.005E_U$, with the regression value of $R^2 = 0.9849$, as depicted in Fig. 8. It is clear that the increase in E_U caused a decrease in E_{dg}. The linear relation between E_{dg} and E_U was observed for other polymer composites and amorphous materials. The increase of the MB concentration in the DPC samples improved the disorder states in the film structure resulting an increase in the E_U in the bandgap,

consequently reducing the E_{dg} values of the MC-MB DPC films, as shown in Fig. 7.

Moreover, Urbach has proposed another formula that correlates the absorption coefficient (α) to the optical energy gap and temperature. This formula is as follows:

$$\alpha = \beta \exp\left[\frac{\sigma(h\nu - E_o)}{K_B T}\right] \tag{4}$$

where β is a pre-exponential constant, σ is the steepness parameter of the Urbach energy, and E_o is the transition energy. For direct transitions, $E_o = E_{dg}$, whereas for indirect transitions, $E_o = E_{ig} \pm E_{ph}$, where E_{ig} and E_{ph} are respectively indirect optical band gap and the associated phonon energy. Consequently, for the present DPC films, Eq. 3 can be rewritten in the logarithmic form as:

$$\ln \alpha = \ln \beta - \frac{\sigma E_{dg}}{K_B T} + \frac{\sigma h\nu}{K_B T} \tag{5}$$

If Eqs. 3 and 5 are compared, the following relations can be deduced:

$$\ln \alpha_o = \ln \beta - \frac{\sigma E_{dg}}{K_B T} \tag{6}$$

and

$$\frac{1}{E_U} = \frac{\sigma}{K_B T} \tag{7}$$

As a result, the steepness parameter (σ) can be evaluated using Eq. 7. The value of σ is also related to the strength of the electron–phonon interaction (E_{e-ph}) by $E_{e-ph} = 2/(3\sigma)$.[31]

The dependency of the steepness parameter (σ) and the electro–phonon interaction (E_{e-ph}) on the MB content in the MC matrix is depicted in Fig. 9. It can be seen that by increasing MC concentration, the σ values decreased while the values of E_{e-ph} enhanced. This could be owing to a change in the coordination number caused by the addition of MC dye, as well as a structural alteration in the system.

Dispersion Behavior of the Refractive Index

Figure 10 presents the spectral behavior of the refractive index $n(\lambda)$ for the MC-MB DPC films with a variety of MB concentrations. The results show that the n varies exponentially with λ, however, its behavior remains roughly unchanged at higher wavelengths (>700 nm), which indicates that the film has a normal dispersion behavior. On the other hand, it is found that as the MB concentration increased in the MC matrix, the n value increased. This result is in agreement with the different empirical models
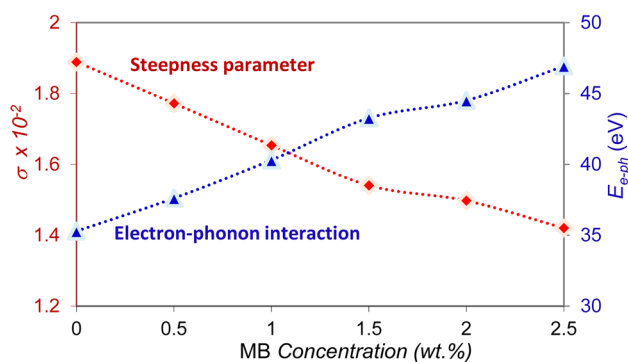
Fig. 9. Variation of the steepness parameter and the electron-phonon interaction with MB content in the MC-MB DPC films.

Fig. 11. The variation of $1/(n^2 - 1)$ versus E^2 and λ^2 for MC-MB DPC films with a variety of MB concentrations.

Table I. The dispersive oscillator parameters according to Wemple–DiDomenico and Sellmeier models.

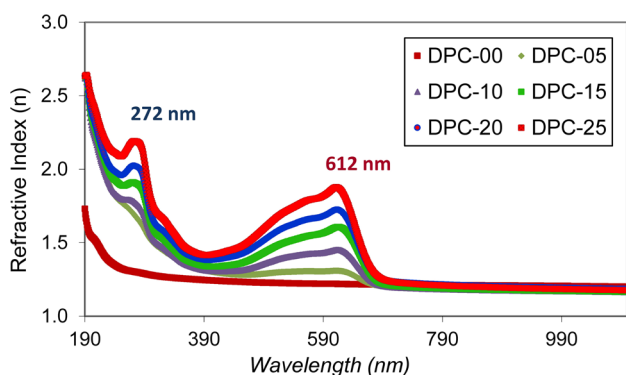| Samples	Wemple–DiDomenico model			Sellmeier model	
	E_o (eV)	E_d (eV)	n_o	S_o (nm^{-2})	λ_o (nm^2)
DPC-00	7.175	3.707	1.236	26.596	0.139
DPC-05	7.075	7.766	1.448	54.945	0.136
DPC-10	6.942	9.464	1.504	70.922	0.133
DPC-15	6.880	12.321	1.601	97.087	0.127
DPC-20	6.776	17.007	1.714	149.254	0.114
DPC-25	6.671	24.046	1.867	232.558	0.103

Fig. 10. Spectral behavior of n for MC-MB DPC films with a variety of MB concentrations.

that correlate the decrease in optical energy bandgap with the increase in refractive index.[36–38]

The single oscillator model (the so-called Wemple-DiDomenico (WDD) model) was used to investigate the dispersion of the refractive index for prepared DPC films:[39]

$$n^2 = 1 + \frac{E_d E_o}{E_o^2 - (h\nu)^2} \tag{8}$$

where E_o and E_d are, respectively, the oscillator energy, and dispersion energy of the system. The values of dispersive oscillator parameters E_o and E_d were calculated accurately from the slope $(-1/E_o E_d)$ and the intersection of extrapolating the linear portion (E_o/E_d) of the plot between $1/(n^2 - 1)$ and $(h\nu)^2$ as shown in Fig. 11, and the results were tabulated in Table I.

The given parameters in Table I reveal that an increase in MB content caused a decrease in E_o and an increase in E_d. Since the value of E_o is interconnected with the bandgap energy, the drop in E_o is due to the observed reduction in E_{gd} due to the increase of MB in the MC matrix. On
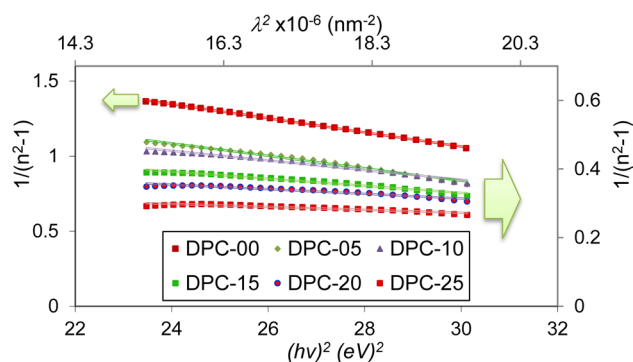
the other hand, the empirical investigation shows a strong correlation between E_d and the strength of the interband optical transition of the thin film.[40] Therefore, the increase in the E_d upon an increase in MB content is assigned to the formation of a charge-transfer complex between MC and MB. Also, the static $(\lambda = 0)$ refractive index (n_o) for the present DPC films is calculated from the relation $n_o = \sqrt{1 + E_d/E_o}$, which is correlated to the static dielectric constant as $(\varepsilon_o = n_o^2)$. It can be noted from Table I that the value of n_o increase with an increase in MB content. It was widely reported that the linear relation between n_o and the volume fraction of additives for various polymer composite systems is an indication that the additive particles are well-dispersed in the host matrix.[29,41,42] Thus, the linear relationship between n_o and MB content in the present study indicates that MB dispersion in the host MC matrix is homogeneous.

Further analysis of refractive index dispersion was performed using a single Sellmeier oscillator to determine the value of the average oscillator strength S_o and the average interband oscillator wavelength λ_o using the following equation:[43]

$$n^2 = 1 + \frac{S_o \lambda_o^2}{1 - \left(\lambda_o/\lambda\right)^2} \tag{9}$$

The values of dispersive oscillator parameters S_o and λ_o are calculated, respectively, from the slope $(-1/S_o)$ and x-intercept $(1/S_o\lambda_o^2)$ of the plots of the variation of $1/(n^2 - 1)$ versus λ^2 for MC-MB DPC films shown in Fig. 11.

Table I summarizes an increase in the calculated value of S_o and a decrease in λ_o as MB concentration increases in the host MC matrix. The results are in accordance with those reported in the literature for other polymer nanocomposites.[44,45] The analysis reveals that the optical energy gap and dispersive oscillator parameters of MC can be fine-tuning by incorporating MB into the matrix. Therefore, these characteristics should, in principle, make MC-MB DPC a potential candidate for optoelectronic device applications.

Nonlinear Optical Parameters

The improvement of the nonlinear (NL) optical performance is critical for lowering power and reducing the lengths of interaction required for many applications. Subsequently, NL optical parameters, such as NL refractive index (η_2) and third-order NL optical susceptibility ($\chi^{(3)}$) play an important role in the fabrication and design of optoelectronic and photonic devices.[43] The $\chi^{(3)}$ is regarded to be the key term of the NL polarization of the material. The following formula is used to determine the $\chi^{(3)}$, using the previously calculated values of dispersive oscillator parameters E_o and E_d:[46]

$$\chi^{(3)} = A \left[\frac{E_o E_d}{4\pi\left(E_o^2 - (h\nu)^2\right)}\right]^4 \tag{10}$$

where $A = 1.7 \times 10^{-10}$ esu is a frequency-independent constant. In addition, the $\chi^{(3)}$ is also related to the NL refractive index η_2 and the static refractive index n_o through the following equation:[47]

$$\eta_2 \left(\frac{cm^2}{W}\right) = \frac{12\pi^2}{n_o^2 c} 10^7 \chi^{(3)}(esu) = \frac{0.0395}{n_o^2} \chi^{(3)}(esu) \tag{11}$$

where $\chi^{(3)}$ is in electrostatic units (esu), i.e. cm^2 statvolt^{-2}. Thus, to investigate the possibility of using MB-doped MC film with different MB content in the optoelectronic device's application, the NL optical parameters $\chi^{(3)}$ and η_2 are computed using the calculated values of dispersive oscillator parameters E_o, E_d and n_o, given in Table I.

The variation of $\chi^{(3)}$ and η_2 against incident photon energy for MC-MB DPC films with various MB content is shown in Fig. 12. It was obvious that the values of $\chi^{(3)}$ and η_2 of the MC-MB DPC films increase with the increases in

MB content in the MC matrix. The increase in both $\chi^{(3)}$ and η_2 might be attributed to alterations in the electronic band structure of MC as a result of the reduction in the optical band gap of DPC films upon incorporating MB dye. It is worth noting that the η_2 values are equivalent to those of oxide glass with heavy metals used in NL fiber optics.[48] It is concluded that the observed increase in the NL optical parameters of MC upon the addition of MB makes it a promising candidate for optoelectronic and photonic device applications.

Conclusion

DPC films of MC-MB systems with various photosensitizer MB contents were developed using a solution casting-evaporation technique. Optical absorption studies reveal that there is a shift in the absorption edge toward the higher wavelengths by the addition of more MB. The direct optical energy gap values have decreased from 6.29 eV for pure MC to 5.95 eV when incorporated with 2.5 wt.% of MB as a result of an increase in the disorder, which increases the defect state density of DPC samples. The relation between Urbach parameters and MB content in the MC matrix was
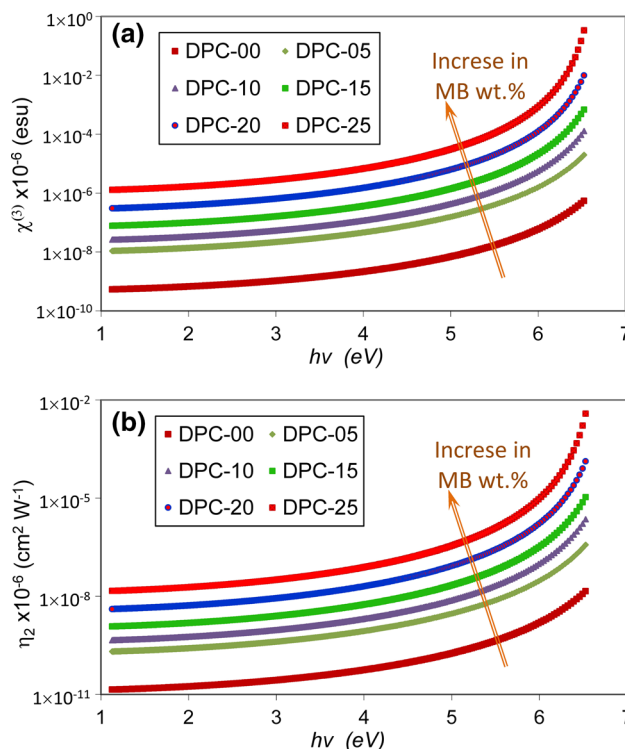

Fig. 12. The dependence of NL optical parameters $\chi^{(3)}$ (a), and η_2 (b), on the incident photon energy ($h\nu$) for MC-MB DPC films with various MB content.

also studied. The nonlinear optical parameters of the present DPC are found to increase significantly with MB content, making MC-MB DPC a potential candidate for optoelectronic and photonic devices.

Declarations

Conflict of interest On behalf of all authors, the corresponding author states that there is no conflict of interest.

References

1. Z.A. Alrowaili, M. Ezzeldien, M.I. Mohammed, and I.S. Yahia, Design of a low-cost laser CUT-OFF filters using carmine dye-doped PVA polymeric composite films. *Results Phys.* 18, 103203 (2020).

2. O.G. Abdullah, Y.A.K. Salman, and S.A. Saleem, Electrical conductivity and dielectric characteristics of in situ prepared PVA/HgS nanocomposite films. *J. Mater. Sci. Mater. Electron.* 27, 3591 (2016).

3. F.J. Hameed, I.M. Ibrahim, O.G. Abdullah, and M.H. Suhai, Enhancing optical and electrical gas sensing properties of polypyrrole nanoplate by dispersing nano-sized tungsten oxide. *ECS J. Solid State Sci. Technol.* 10, 107001 (2021).

4. M.M. Abdelhamied, A. Atta, A.M. Abdelreheem, A.T.M. Farag, and M.M. El Okr, Synthesis and optical properties of PVA/PANI/Ag nanocomposite films. *J. Mater. Sci. Mater. Electron.* 31, 22629 (2020).

5. O.G. Abdullah, and S.A. Saleem, Effect of copper sulfide nanoparticles on the optical and electrical behavior of poly (vinyl alcohol) films. *J. Electron. Mater.* 45, 5910 (2016).

6. V. Hebbar, R.F. Bhajantri, J. Naik, and S.G. Rathod, Thiazole yellow G dyed PVA films for optoelectronics: microstructrural, thermal and photophysical studies. *Mater. Res. Express* 3, 075301 (2016).

7. A.F. Abdulameer, M.H. Suhail, O.G. Abdullah, and I.M. Al-Essa, Fabrication and characterization of NiPcTs organic semiconductors based surface type capacitive-resistive humidity sensors. *J. Mater. Sci. Mater. Electron.* 28, 13472 (2017).

8. T.A. Skotheim, J.R. Reynolds, and B.C. Thompson, *Handbook of Conducting Polymers-Conjugated Polymers: Properties, Processing and Applications* (CRC Press, Taylor & Francis Group, 2019).

9. S. Sreedhar, N. Illyaskutty, S. Sreedhanya, R. Philip, and C.I. Muneera, An organic dye-polymer (phenol red-poly (vinyl alcohol)) composite architecture towards tunable -optical and -saturable absorption characteristics. *J. Appl. Phys.* 119, 193106 (2016).

10. D. Ghoshal, D. Bhattacharya, D. Mondal, S. Das, N. Bose, and M. Basu, Methylene blue/PVA composite film for flexible, wide-scale UV–VIS laser cut-off filter. *Mater. Res. Express* 6, 075332 (2019).

11. H.T. Ahmed, and O.G. Abdullah, Preparation and composition optimization of PEO:MC polymer blend films to enhance electrical conductivity. *Polymers* 11, 853 (2019).

12. P.L. Nasatto, F. Pignon, J.L.M. Silveira, M.E.R. Duarte, M.D. Noseda, and M. Rinaudo, Methylcellulose, a cellulose derivative with original physical properties and extended applications. *Polymers* 7, 777 (2015).

13. O.G. Abdullah, H.T. Ahmed, D.A. Tahir, G.M. Jamal, and A.H. Mohamad, Influence of PEG plasticizer content on the proton-conducting PEO:MC-NH4I blend polymer electrolytes based films. *Results Phys.* 23, 104073 (2021).

14. R. Begum, J. Najeeb, A. Sattar, K. Naseem, A. Irfan, A.G. Al-Sehemi, and Z.H. Farooqi, Chemical reduction of methylene blue in the presence of nanocatalysts: a critical review. *Rev. Chem. Eng.* 36, 749 (2020).

15. O.G. Abdullah, Y.A.K. Salman, D.A. Tahir, G.M. Jamal, H.T. Ahmed, A.H. Mohamad, and A.K. Azawy, Effect of ZnO nanoparticle content on the structural and ionic transport parameters of polyvinyl alcohol based proton–conducting polymer electrolyte membranes. *Membranes* 11, 163 (2021).

16. M.H. Suhail, O.G. Abdullah, and G.A. Kadhim, Hydrogen sulfide sensors based on PANI/f–SWCNT polymer nanocomposite thin films prepared by electrochemical polymerization. *J. Sci. Adv. Mater. Dev.* 4, 143 (2019).

17. O.G. Abdullah, D.A. Tahir, and K. Kadir, Optical and structural investigation of synthesized PVA/PbS nanocomposites. *J. Mater. Sci. Mater. Electron.* 26, 6939 (2015).

18. V.P. Dinh, T.D.T. Huynh, H.M. Le, V.D. Nguyen, V.A. Dao, N.Q. Hung, L.A. Tuyen, S. Lee, J. Yi, T.D. Nguyen, and L.V. Tan, Insight into the adsorption mechanisms of methylene blue and chromium(III) from aqueous solution onto pomelo fruit peel. *RSC Adv.* 9, 25847 (2019).

19. R. Zuo, G. Du, W. Zhang, L. Liu, Y. Liu, L. Mei, and Z. Li, Photocatalytic degradation of methylene blue using TiO2 impregnated diatomite. *Adv. Mater. Sci. Eng.* 2014, 170148 (2014).

20. T.A. Devi, N. Ananthi, and T.P. Amaladhas, Photobiological synthesis of noble metal nanoparticles using Hydrocotyle asiatica and application as catalyst for the photodegradation of cationic dyes. *J. Nanostruct. Chem.* 6, 75 (2016).

21. A.H. Mohamad, S.R. Saeed, and O.G. Abdullah, Synthesis of very–fine PbS nanoparticles dispersed homogeneously in MC matrix: effect of concentration on the structural and optical properties of the host polymer. *Mater. Res. Express* 6, 115332 (2019).

22. O.G. Abdullah, R.R. Hanna, and Y.A.K. Salman, Structural and electrical conductivity of CH:MC bio–poly–blend films: Optimize the perfect composition of the blend system. *Bull. Mater. Sci.* 42, 64 (2019).

23. S. Gao, R. Cao, and C. Yang, Dye–polyoxometalate composite films: self-assembly, thermal and photochemical properties. *J. Colloid. Interf. Sci.* 324, 156 (2008).

24. R.T. Abdulwahid, O.G. Abdullah, S.B. Aziz, S.A. Hussein, F.F. Muhammad, and M.Y. Yahya, The study of structural and optical properties of PVA:PbO2 based solid polymer nanocomposites. *J. Mater. Sci. Mater. Electron.* 27, 12112 (2016).

25. A.S. Hassanien, and A.A. Akl, Effect of Se addition on optical and electrical properties of chalcogenide CdSSe thin films. *Superlattice Microstruct.* 89, 153 (2016).

26. R.N. Abed, E. Yousif, A.R.N. Abed, A.A. Rashad, A. Hadawey, and A.H. Jawad, Optical properties of PVC composite modified during light exposure to give high absorption enhancement. *J. Non-Cryst. Solids* 570, 120946 (2021).

27. J. Tauc, *Amorphous and Liquid Semiconductors* (New York: Plenum, 1974).

28. N.F. Mott, and E.A. Davis, *Electronic Processes in Non-crystalline Materials* (Oxford: Clarendon Press, 1979).

29. O.G. Abdullah, S.B. Aziz, and M.A. Rasheed, Effect of silicon powder on the optical characterization of poly(methyl methacrylate) polymer composites. *J. Mater. Sci. Mater. Electron.* 28, 4513 (2017).

30. O.G. Abdullah, R.R. Hanna, and Y.A.K. Salman, Structural, optical, and electrical characterization of chitosan: methylcellulose polymer blends based film. *J. Mater. Sci. Mater. Electron.* 28, 10283 (2017).

31. F. Urbach, The long-wavelength edge of photographic sensitivity and of the electronic absorption of solids. *Phys. Rev.* 92, 1324 (1953).

32. O.G. Abdullah, B.K. Aziz, S.B. Aziz, and M.H. Suhail, Surfaces modification of methylcellulose: cobalt nitrate polymer electrolyte by sulfurated hydrogen gas treatment. *J. Appl. Polym. Sci.* 135, 46676 (2018).

33. A. Shubha, and S.R. Manohara, Effect of graphene nanoplatelets concentration on optical, dielectric and electrical properties of poly(2-ethyl-2-oxazoline)–polyvinylpyrrolidone–graphene nanocomposites. *J. Mater. Sci. Mater. Electron.* 31, 16498 (2020).

34. S.F. Bdewi, O.G. Abdullah, B.K. Aziz, and A.A.R. Mutar, Synthesis, structural and optical characterization of MgO nanocrystalline embedded in PVA matrix. *J. Inorg. Organomet. Polym. Mater.* 26, 326 (2016).

35. O.G. Abdullah, Synthesis of single-phase zinc chromite nano-spinel embedded in polyvinyl alcohol films and its effects on energy band gap. *J. Mater. Sci. Mater. Electron.* 27, 12106 (2016).

36. P.J.L. Herve, and L.K.J. Vandamme, Empirical temperature dependence of the refractive index of semiconductors. *J. Appl. Phys.* 77, 5476 (1995).

37. N.M. Ravindra, S. Auluck, and V.K. Srivastava, On the Penn gap in semiconductors. *Phys. Status Solidi B* 93, K155 (1979).

38. M.I. Amer, S.H. Moustafa, and M. El-Hagary, Enhanced band structure, optoelectronic and magnetic properties of spray pyrolysis Ni-doped SnO2 nanostructured films. *Mater. Chem. Phys.* 248, 122892 (2020).

39. S.H. Wemple, and M. DiDomenico, Behavior of the electronic dielectric constant in covalent and ionic materials. *Phys. Rev. B* 3, 1338 (1971).

40. O.G. Abdullah, S.B. Aziz, K.M. Omer, and Y.M. Salih, Reducing the optical band gap of polyvinyl alcohol (PVA) based nanocomposite. *J. Mater. Sci. Mater. Electron.* 26, 5303 (2015).

41. P. Tao, Y. Li, A. Rungta, A. Viswanath, J. Gao, B.C. Benicewicz, R.W. Siegel, and L.S. Schadler, TiO2 nanocomposites with high refractive index and transparency. *J. Mater. Chem.* 21, 18623 (2011).

42. J. Jin, R. Qi, Y. Su, M. Tong, and J. Zhu, Preparation of high-refractive-index PMMA/TiO2 nanocomposites by one-step in situ solvothermal method. *Iran. Polym. J.* 22, 767 (2013).

43. M. El-Hagary, S.H. Moustafa, M.I. Amer, G.M.A. Gad, M.E. Ismail, and H. Hashem, Linear, non-linear optical properties and magnetic studies of spray pyrolysis nanocrystalline Sn1-xCoxO2 films for multifunctional optoelecronic and spintronic applications. *J. Mater. Res. Technol.* 13, 2310 (2021).

44. T.A. Hameed, F. Mohamed, A.M. Abdelghany, and G. Turky, Influence of SiO2 nanoparticles on morphology, optical, and conductivity properties of poly (ethylene oxide). *J. Mater. Sci. Mater. Electron.* 31, 10422 (2020).

45. A. Atta, M.M. Abdelhamied, A.M. Abdelreheem, and M.R. Berber, Flexible methyl cellulose/polyaniline/silver composite films with enhanced linear and nonlinear optical properties. *Polymers* 13, 1225 (2021).

46. H. Ticha, and L. Tichy, Semiempirical relation between non-linear susceptibility (refractive index), linear refractive index and optical gap and its application to amorphous chalcogenides. *J. Optoelectron. Adv. Mater.* 4, 381 (2002).

47. R.W. Boyd, *Nonlinear Optics*, 3rd ed., (Amsterdam: Elsevier Science, 2008).

48. J. Cimek, N. Liaros, S. Couris, R. Stepien, M. Klimczak, and R. Buczynski, Experimental investigation of the nonlinear refractive index of various soft glasses dedicated for development of nonlinear photonic crystal fibers. *Opt. Mater. Express* 7, 3471 (2017).